Genetic architecture of zinc hyperaccumulation in *Arabidopsis halleri*: the essential role of QTL × environment interactions

Hélène Frérot[1], Michel-Pierre Faucon[1], Glenda Willems[1], Cécile Godé[1], Adeline Courseaux[1], Aude Darracq[1], Nathalie Verbruggen[2] and Pierre Saumitou-Laprade[1]

[1]Laboratoire de Génétique et Evolution des Populations Végétales, UMR CNRS 8016, Université des Sciences et Technologies de Lille - Lille1, F-59655 Villeneuve d'Ascq Cedex, France; [2]Laboratoire de Physiologie et de Génétique Moléculaire des Plantes, Université Libre de Bruxelles, Campus de la Plaine, CP242, boulevard du Triomphe, 1050 Bruxelles, Belgium

Author for correspondence:
Hélène Frérot
Tel: +33 3 20 43 40 33
Email: helene.frerot@univ-lille1.fr

Received: *27 January 2010*
Accepted: *6 April 2010*

New Phytologist (2010) **187**: 355–367
doi: 10.1111/j.1469-8137.2010.03295.x

Key words: *Arabidopsis halleri*, hyperaccumulation, QTL × environment interactions, QTL mapping, zinc (Zn).

Summary

- This study sought to determine the main genomic regions that control zinc (Zn) hyperaccumulation in *Arabidopsis halleri* and to examine genotype × environment effects on phenotypic variance. To do so, quantitative trait loci (QTLs) were mapped using an interspecific *A. halleri* × *Arabidopsis lyrata petraea* F_2 population.
- The F_2 progeny as well as representatives of the parental populations were cultivated on soils at two different Zn concentrations. A linkage map was constructed using 70 markers.
- In both low and high pollution treatments, zinc hyperaccumulation showed high broad-sense heritability (81.9 and 74.7%, respectively). Five significant QTLs were detected: two QTLs specific to the low pollution treatment (chromosomes 1 and 4), and three QTLs identified at both treatments (chromosomes 3, 6 and 7). These QTLs explained 50.1 and 36.5% of the phenotypic variance in low and high pollution treatments, respectively. Two QTLs identified at both treatments (chromosomes 3 and 6) showed significant QTL × environment interactions.
- The QTL on chromosome 3 largely colocalized with a major QTL previously identified for Zn and cadmium (Cd) tolerance. This suggests that Zn tolerance and hyperaccumulation share, at least partially, a common genetic basis and may have simultaneously evolved on heavy metal-contaminated soils.

Introduction

Metal hyperaccumulation in plants is the capacity to concentrate high amounts of certain metals in the shoots without suffering from toxicity symptoms (Baker, 1981; Baker & Brooks, 1989; Reeves & Baker, 2000). In metallophyte or pseudometallophyte species, all or some populations can successfully grow and reproduce on heavy metal-contaminated soils (the so-called 'metal tolerance'; Antonovics *et al.*, 1971; Macnair, 1983). Only a few species are able to accumulate metals in their aerial parts (Baker & Brooks, 1989; Baker *et al.*, 2000; Broadley *et al.*, 2001). Whether hyperaccumulation is an adaptive trait to extreme metallic environments is still elusive, as many hypotheses of adaptive function have been proposed. Hyperaccumulation may be a mechanism of metal detoxification and tolerance, metal removal from the rhizosphere for further elimination by defoliation or rainfall action, drought resistance, allelopathy, the by-product of a mechanism that has another adaptive function (often called 'inadvertent uptake hypothesis'), or protection against herbivores or pathogens (summarized in Boyd & Martens, 1992). To date, however, none of these hypotheses have been able to completely elucidate the origin of metal hyperaccumulation (Whiting *et al.*, 2003; Noret *et al.*, 2005). Hyperaccumulation is also interesting from an environmental or agronomic point of view. In mining or industrial sites and their surroundings, heavy metals are responsible for severe and unhealthy soil contamination. In these cases, hyperaccumulating plants could be used as biological tools for phytoremediation techniques as they may

help remove metals from soils (Salt *et al.*, 1995, 1998; Pilon-Smits, 2005). Since some heavy metals are also essential minerals that can be deficient in staple food crops, genetic determinants of hyperaccumulation could be utilized in biofortification with the aim of improving the nutritional value of these crops (Cakmak, 2008; Jeong & Guerinot, 2008; Mayer *et al.*, 2008; Palmgren *et al.*, 2008). Since metal hyperaccumulation is of both fundamental and applied interest, the mechanisms underlying this trait thus deserve to be understood, from root uptake to vacuolar sequestration, via xylem loading, translocation to shoots, and xylem unloading to leaf cells (for review, see Clemens, 2001, 2006; Verbruggen *et al.*, 2009). Over the past few years, the genetics of metal accumulation has benefited from the development of molecular tools (Verbruggen *et al.*, 2009). Transcriptomic analyses comparing hyperaccumulator and nonaccumulator species has revealed that many genes are involved in hyperaccumulation and show different expression profiles or regulation-level modifications (Becher *et al.*, 2004; Weber *et al.*, 2004; Filatov *et al.*, 2006; van de Mortel *et al.*, 2006, 2008; Talke *et al.*, 2006).

Arabidopsis halleri is a pseudometallophyte of the Brassicaceae family. This species has been described as cadmium (Cd)-tolerant, constitutively zinc (Zn)-tolerant as well as Zn-hyperaccumulating (Bert *et al.*, 2000, 2002, 2003; Macnair, 2002; Pauwels *et al.*, 2006). While metallicolous populations tend to show higher Zn tolerance than nonmetallicolous populations (Pauwels *et al.*, 2006), they also display lower hyperaccumulation capacities in controlled conditions than nonmetallicolous populations (Bert *et al.*, 2000). Being a close relative of *Arabidopsis thaliana*, with which it shows roughly 94% nucleotide identity within coding regions (Becher *et al.*, 2004), *A. halleri* is an excellent model species for studying metal tolerance and hyperaccumulation (Pauwels *et al.*, 2008a,b; Roosens *et al.*, 2008a,b). Using first-generation backcross progeny (BC1) from an interspecific cross between *A. halleri* and *Arabidopsis lyrata petraea*, a nontolerant and nonaccumulator relative, quantitative trait locus (QTL) analyses have been performed for Zn (Willems *et al.*, 2007) and Cd tolerance (Courbot *et al.*, 2007). A major QTL region common to Zn and Cd tolerance has been identified, colocalizing with *HMA4*, a gene encoding a heavy metal-transporting ATPase. The importance of this gene was recently confirmed with functional studies using RNAi-mediated silencing (Hanikenne *et al.*, 2008). *A. halleri* plants with reduced expression of *HMA4* translocate less Zn from roots to shoots, while *A. thaliana* plants expressing *AhHMA4* show an increase in shoot Zn accumulation. However, because these transgenic *A. thaliana* plants showed signs of Zn hypersensitivity in shoots (Hanikenne *et al.*, 2008), *AhHMA4* expression alone is not sufficient to detoxify Zn. Additional genes are thus required to completely understand Zn hyperaccumulation in *A. halleri*.

In this study, to identify the main genomic regions responsible for Zn hyperaccumulation in *A. halleri*, QTL mapping was performed on F_2 progeny from an *A. halleri* and *A. lyrata petraea* cross. In *A. halleri*, Zn hyperaccumulation variability depends on external Zn concentrations (Macnair, 2002), which implies that variation in Zn hyperaccumulation may – in part – correspond to a genotype × environment interaction. This type of interaction was tested in this study by cultivating the same F_2 progeny at different Zn concentrations. Since it has been demonstrated that interactions among genes (i.e. epistasis) are also involved in genetic architecture of adaptive traits (Malmberg & Mauricio, 2005), epistasis was also evaluated here. Additionally, based on a large set of markers common to the *A. halleri* × *A. lyrata petraea* BC1 map and the F_2 linkage map, the genomic regions detected for Zn : Cd tolerance and Zn (this paper) or Cd (Willems *et al.*, 2010) hyperaccumulation were compared. Finally, taking advantage of the high synteny between the *A. halleri* and the *A. thaliana* genomes (Roosens *et al.*, 2008a,b), putative candidate genes for Zn hyperaccumulation were proposed.

Materials and Methods

Plant material

Arabidopsis halleri (L.) O'Kane et Al-Shehbaz individuals originated from an industrial calamine site in the north of France contaminated with Zn, Cd and lead (Auby, France) (Van Rossum *et al.*, 2004), and *A. lyrata petraea* individuals came from a nonpolluted site in the Czech Republic (Unhošt', Central Bohemia) (Macnair *et al.*, 1999). Both species have a haploid set of eight chromosomes. They are self-incompatible. Hence, to avoid inbreeding depression effect, two randomly selected *A. halleri* (pollen donor) individuals and two randomly selected *A. lyrata petraea* (pollen recipient) individuals were necessary to produce two independent F_1 progeny. Two randomly selected F_1 plants from each cross were used to generate F_2 populations, and the F_2 progeny presenting the largest seed number (roughly 300) was selected. The F_2 population used for linkage map construction consisted of 288 individuals, of which 208 were analyzed for Zn accumulation. F_2 genotypes were duplicated and maintained in time by cuttings. As cuttings of parental and F_1 plants died before they could be analyzed, individuals from the same population (n = 4 for *A. halleri* and n = 3 for *A. lyrata petraea*) or generation (n = 8 for F_1) were used in this study.

Plant cultivation and evaluation of Zn hyperaccumulation

All plants were grown individually in 1 l pots containing compost, in a glasshouse environment (temperature, 20°C

day : 15°C night; photoperiod, 14 h day : 10 h night). The photoperiod was adjusted by 400 W high-pressure sodium lamps, photosynthetically active radiation (PAR) of 90 μM photons m^{-2} s^{-1} over the wavelength range 400–700 nm; the lamps were automatically switched off when daylight was sufficiently intense. Plants were watered every 2 d with deionized water. After 6 months of cultivation, leaves were collected for DNA extraction.

Several cuttings of each genotype were produced so as to obtain six replicates of the same genotype. Three replicates were grown in a 'low pollution' (LP) treatment consisting of compost with no added Zn. Total Zn concentration in an LP treatment corresponded to 15 mg kg^{-1} dry matter, while available Zn concentration corresponded to 8 mg kg^{-1} dry matter. The three other replicates were grown in a 'high pollution' (HP) treatment consisting of a soil contaminated with 50 ml of a 100 mM ($ZnSO_4$, $7H_2O$) solution added to 650 g of fresh compost, 2 d before transplantation to allow restoration of equilibrium between soil elements. Total Zn concentration was, in this case, 1500 mg kg^{-1} dry matter, while available Zn concentration was 1200 mg kg^{-1} dry matter. This concentration was selected because it ensured complete survival and sufficient growth of all plants, as it corresponded to a low amount of pollution in comparison to that in metalliferous sites (Bert *et al.*, 2002; Meyer *et al.*, 2010). Environmental heterogeneity was controlled by a weekly rotation of the 1248 pots. After 6 wk of cultivation, the whole rosette of each replicate was harvested, washed twice in demineralized water, dried at 55°C for 72 h, weighted and ground. A 25 mg aliquot was digested in 750 μl of a 2% sulfosalicylic acid solution. After 24 h of digestion, 4 μl of this solution was mixed with 40 μl of 0.03% zincon solution, the colorimetric reagent, and 156 μl of a buffer at pH 9.6 (Macnair & Smirnoff, 1999). Absorbance values were measured at 606 nm on a microplate absorbance reader (SUNRISE Tecan V 3.17, Grödig, Austria). Shoot Zn concentrations were then expressed as mg kg^{-1} shoot dry weight.

Statistical analysis

The arithmetic mean of Zn accumulation for each parental and F_1 representative and each F_2 genotype was calculated from the three replicates in each treatment. On the base of mean value for each F_2 genotype, the Spearman rank correlation between the two treatments (CORR procedure of SAS Institute 2002) and the comparison of means between the two treatments using a paired Student's *t*-test (TTEST procedure of SAS Institute 2002) were computed. A normality test based on the Kolmogorov–Smirnov D statistics (UNIVARIATE procedure of SAS Institute 2002) was also performed (H_0: the distribution data corresponds to a normal distribution). Because of a significant but quite low departure from normality ($D = 0.09$), mainly as a result of extreme values, data were not transformed before analysis of variance (ANOVA). A two-way ANOVA using the GLM procedure in SAS Institute (2002) was performed to determine the treatment and genotype effects and their interaction. The main factor 'genotype' was considered as a random effect, because the F_2 individuals tested for Zn accumulation represent a random sampling of the total F_2 population. Type III sums of squares were used because of unbalanced data sets. Variance components were also estimated using the TYPE 1 method of the VARCOMP procedure of SAS Institute (2002). The broad-sense heritability of Zn accumulation was estimated for each environment using variance components as $H^2 = V_G/V_P$ (Wu & Stettler, 1997; Juenger *et al.*, 2005). V_G is the total genetic variance, which included additive genetic variance and other genetic sources of variance (dominance and epistasis). V_P is the total phenotypic variance calculated as ($V_G + V_{error}$). These two variance components were estimated using the TYPE 1 method of the VARCOMP procedure of SAS Institute (2002), with the 'genotype' factor considered as a random effect.

Quantitative trait locus × environment interactions were tested by two-way analyses of variance by using the GLM procedure of SAS Institute (2002). The models involved two main fixed factors represented by one of the markers 1-04488, 2-08286, 2-15997, 4-17540 (instead of 4-17202 because this marker displayed only two genotype classes), 5-05494 or 5-04824, at QTL positions or closest to the QTL positions, and Zn treatment (HP or LP). In addition, between-QTLs interactions at the corresponding markers were tested using exact nonparametric Kruskall–Wallis tests (StatXact v.7 Cytel Studio 2005, Cambridge, Massachusetts, USA) because sample sizes were very unbalanced (see Supporting Information Table S3).

Development of the markers

The genomic DNA of the four parental genotypes, the two F_1 individuals that were crossed out, and 288 individuals of the F_2 progeny, was extracted using a Kit NucleoSpin 96 Plant (Macherey-Nagel, Hoerdt, France). Seventy markers were selected for genotyping (Table S1). Some of them are derived from genes directly implied in metal homeostasis in either *A. halleri* or *Thlaspi caerulescens* (*Ah-NAS2*, *Ah-CCH*, *Ah-HMA4*, *Ah-NRAMP3*, *Ah-ZIP6*, *Ah-CAX1*, *Ah-MHX1*, *Ah-HMADP2*, *Ah-YSL3*, *Ah-NRAMP4*, and *Tc-UP2*). Details on 44 of these markers (primer sequence and PCR conditions) were described in Willems *et al.* (2007), Courbot *et al.* (2007), Roosens *et al.* (2008a) and Ruggiero *et al.* (2008), as they were previously mapped in the BC1 progeny of *A. halleri* and *A. lyrata petraea*. Two new markers were developed to complete the genetic map in uncovered regions or to replace previously mapped markers that were not polymorphic in the F_2. Marker Chr.5-21773/*Ah-YSL3*, belonging to the Yellow-Stripe-like transporter

family (nicotianamine complex) and chosen for its position on linkage group 8, and marker Chr.3-05134/Lyr133, a microsatellite locus defined in *A. lyrata petraea*, were kindly provided by Dr Tom Mitchell-Olds. These markers were amplified and scored as described in Willems *et al.* (2007) with the specific PCR condition: 50°C annealing temperature for 1 min and 50°C for 45 s, respectively. Twenty-two new microsatellite markers were also produced in this work to increase the coverage of the *A. halleri* genetic map. One microsatellite marker was defined within exon 10 from the *HMA4* sequence (Hanikenne *et al.*, 2008) and included a simple sequence repeat (SSR) motif corresponding to $(CCA)_6$. The other new microsatellite markers were selected from a microsatellite-enriched genomic library developed in the GEPV laboratory following an enrichment procedure with Dynabeads (Glenn & Schable, 2005). *In silico* analysis on sequenced microsatellites were conducted with an in-house program using ClustalW (Larkin *et al.*, 2007) to eliminate sequence redundancy and MREPS (Kolpakov *et al.*, 2003) to find microsatellite patterns. Primer sequences were designed in flanking regions of *A. halleri* microsatellites using Primer3 software (http://frodo.wi.mit.edu/). In order to allow polymerase chain reaction (PCR) multiplexing of markers, primer combinations were chosen with a 60°C (± 5°C) melting temperature, and a PIG-tail (GTGTCTT) was added to the 5′-end region of the reverse primer to facilitate adenylation and avoid stutter bands (Brownstein *et al.*, 1996). To help combination into four fluorescently labelled multiplex groups, allowing the loading of multiplexes, a universal M13 tail (CACGACGTTGTAAAACGAC) was added to the 5′-region of the forward primers.

Multiplex PCR was carried out in 10 μl reactions containing 1× PCR buffer II (Applied Biosystems, Foster City, CA, USA), 2.5 mM $MgCl_2$, 150 nM dNTP (Euromedex, France), 0.075 μM of the Forward-M13 primer, 0.375 μM of the reverse-PIG primer, 1.5 μM of fluorescently dye labelled M13 (Applied Biosystems), 0.5 U of Qiagen Multiplex PCR kit, and 5 μl DNA (20–60 ng). PCRs were conducted on a Mastercycler pro S (Eppendorf, UK). In order to improve the specificity and the quality of amplification, parameters for thermal cycling included two touchdown phases in which the annealing temperature was decreased by 2°C every cycle as follows: 94°C for 5 min followed by first touchdown over five cycles of 45 s at 95°C, 5 min at 68–60°C, 1 min at 72°C, followed by second touchdown over five cycles of 45 s at 95°C, 1 min at 58–50°C, 1 min at 72°C, then 27 cycles of 45 s at 95°C, 30 s at 47°C, 1 min at 72°C, and a final elongation cycle of 10 min at 72°C. Allele sizing of microsatellite multiplex amplified products was performed using an ABI Prism® 3100 Genetic Analyzer 16-capillary array system (Applied Biosystems). The four PCR products labelled with different dyes were mixed and 1.5 μl of the mixture was added to 0.25 μl GeneScan-500 LIZ Size standard and 9.95 μl of HiDi formamide (both products from Applied Biosystems). Fragment sizes were analyzed with GeneMapper Software version 3.7 (Applied Biosystems).

The putative position of microsatellite markers on the *A. thaliana* genome was determined by searching for sequence homology using the BLAST function of NCBI (http://www.ncbi.nlm.nih.gov/). For Ah75 and Ah77 markers, the expected position was not consistent with the observed position on the *A. halleri* map, so that no position was indicated (Table S1).

Linkage analysis and map construction

The *A. halleri* × *A. lyrata petraea* linkage map was constructed using the software package JoinMap 3.0 (Van Ooijen & Voorrips, 2001). Markers that were polymorphic in the parents and in the F_1 displayed from two to four different alleles that could be identified in F_2 progeny. For population type CP ('cross-pollinators'), JoinMap software uses different segregation types corresponding to genotypes of the last parental generation, here the F_1 generation. These segregation types are <abxcd> for four alleles, <efxeg> for three alleles, and <hkxhk>, <lmxll> and <nnxnp> for two alleles. These genotypes are also associated with their linkage phases for both parents during the estimation of recombination frequencies.

The grouping of loci is based upon a test for independence translated into a logarithm of odds (LOD) score. Loci determined to be significantly associated at a reasonable LOD threshold will be in the same group. Then, to order loci on linkage groups, a mapping procedure was used, which is based on a sequential method adding loci one by one and starting from the most informative pair of loci. For each added locus, the best position is sought by comparing the goodness-of-fit of the resulting map for each tested position. The goodness-of-fit measure is a G^2 likelihood ratio statistic that compares all direct recombination frequencies (i.e. the pairwise data based on the original genotype data of the two loci involved) with the map-derived combination frequencies (i.e. calculated with an inverse mapping function). Kosambi's mapping function (Kosambi, 1944) was used to convert recombination frequencies into map distances (cM).

Marker segregation

According to Mendelian inheritance, the allele segregation in the F_2 progeny is expected to fit different ratios depending on the segregation type, that is, 1 : 1 : 1 : 1 for <abxcd> and <efxeg>, 1 : 2 : 1 for <hkxhk>, and 1 : 1 for <lmxll> and <nnxnp>. Deviations from Mendelian expected ratios were performed in JoinMap 3.0 using a chi-square test at a locus-by-locus significance threshold of 5% (Van Ooijen & Voorrips, 2001).

Detection of QTLs

Potential QTLs for each trait (ZnAcLP for 'Zn accumulation in LP treatment' and ZnAcHP for 'Zn accumulation in HP treatment') were detected using the MapQTL 4.0 software (Van Ooijen *et al.*, 2002). A Kruskall–Wallis rank test was first performed on each locus separately to find potential regions of QTL. A segregating QTL closely linked to the tested marker results in a large difference in average rank of the marker genotype classes. Interval mapping (IM) analysis then allowed a finer detection by testing the occurrence of a QTL and computing a LOD score for every centiMorgan (cM) along the linkage groups. The LOD score represents the 10-base logarithm of the quotient of two likelihoods: the likelihood of the presence of a segregating QTL (alternative hypothesis) divided by the likelihood of no segregating QTL (null hypothesis). To declare the occurrence of a QTL, the calculated LOD scores were compared with a LOD score threshold obtained by a permutation test (1000 permutations), which corresponds to a genome-wide empirical significance threshold at the 5% level (Churchill & Doerge, 1994). In this way the threshold value was set at 4.0 for each trait. A Multiple-QTL Model (MQM) analysis was finally performed every cM, in which markers close to detected QTLs (by IM mapping) were selected as cofactors to take over the role of the nearby QTLs in the approximate multiple-QTL models used in the subsequent MQM analysis. This method reduces the residual variance and enhances the power of searching for other segregating QTLs. It also improves the precision of QTL positions. After manual selection of cofactors, an automatic selection of cofactors was executed to keep a restricted set of significant cofactors. MQM mapping was thus performed again using this new set of cofactors to obtain the best possible QTL positions and maximal LOD scores. The threshold LOD score was maintained at 4.0 for each trait. The LOD score profiles showing QTLs with their one- and two-LOD support intervals were obtained using MapChart 2.1 (Voorrips, 2002).

Additive effects (a) of the QTL were calculated as follows: $(\mu_{lyr1/lyr2} - \mu_{hal1/hal2})/2$, where $\mu_{hal1/hal2}$ and $\mu_{lyr1/lyr2}$ are the mean concentrations for the homospecific genotypes *halleri*-1/*halleri*-2 and *lyrata*-1/*lyrata*-2 at the markers closest to or at the QTL. Two heterospecific genotype classes (*halleri*-1/*lyrata*-2 and *halleri*-2/*lyrata*-1) can be distinguished at the QTL in this mapping population. Therefore, dominance effects (d) at the QTL correspond to either $(\mu_{hal1/lyr2} - (\mu_{hal1/hal2} + \mu_{lyr1/lyr2})/2)$ or $(\mu_{hal2/lyr1} - (\mu_{hal1/hal2} + \mu_{lyr1/lyr2})/2)$, where $\mu_{hal1/lyr2}$ and $\mu_{hal2/lyr1}$ are the mean concentrations of the genotypes that are heterospecific *halleri*-1/*lyrata*-2 and *halleri*-2/*lyrata*-1, respectively, at the QTL. All the mean concentrations were estimated by the MQM method implemented in MapQTL. The degree of dominance at the QTL is obtained by the ratio $|d/a|$. According to the degree of dominance, QTLs were classified as additive ($|d/a| < 0.2$), partially dominant ($0.2 \leq |d/a| < 0.8$), dominant ($0.8 \leq |d/a| < 1.2$), or overdominant ($|d/a| \geq 1.2$) (Stuber *et al.*, 1987).

Results

Trait heritability and segregation

In LP and HP treatments, the broad-sense heritabilities estimated as a percentage of total phenotypic variance were high: 81.9 and 74.7%, respectively.

Zinc accumulation values in the LP treatment were distributed between 176 and almost 3000 mg kg^{-1} among the F_2 progeny, while in the HP treatment they were widely distributed from almost 1000 to 9196 mg kg^{-1} (Fig. 1). All the *A. lyrata petraea* representatives fell in the lowest phenotype class, whereas the *A. halleri* representatives and F_1 progeny showed a larger distribution. Some F_1 progeny were phenotypically close to *A. lyrata petraea*, indicating that Zn accumulation was partially recessive in *A. halleri*. Because parents' representatives were not the

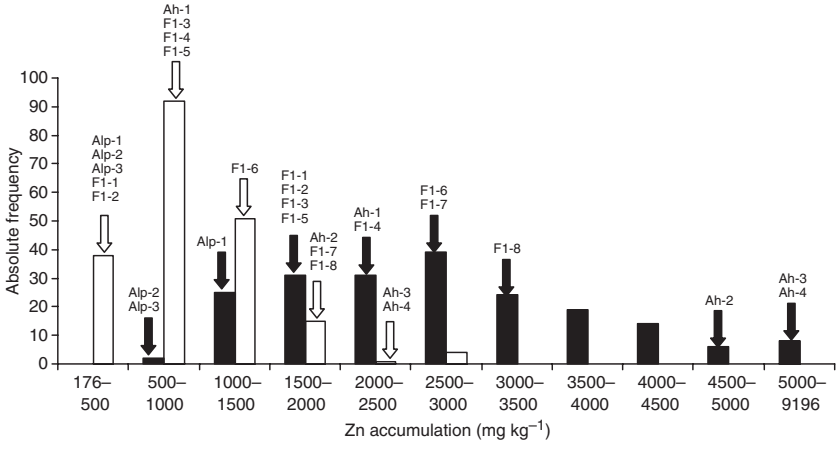

Fig. 1 Segregation profiles of Zn accumulation in the 'low pollution' treatment (white bars) and the 'high pollution' treatment (black bars). Parents' representatives are noted above the arrows to give their phenotype class. Alp, representatives of *Arabidopsis lyrata petraea*; Ah, representatives of *Arabidopsis halleri*; F_1, representatives of F_1 progeny.

original parents, it was not possible to evaluate phenotypic transgression effectively. Nevertheless, only four F_2 individuals in the LP treatment and two F_2 individuals in the HP treatment showed higher accumulation values than *A. halleri* individuals (data not shown). In addition, it is worth noting that in the two soil treatments, the *A. halleri* individuals displayed different phenotypic values for accumulation. This suggests that Zn accumulation capacity is not fixed in the species. The two segregation profiles did not correspond to a normal distribution ($D = 0.09$, $P < 0.01$ for both LP and HP). Nevertheless, the skewness (1.4) and kurtosis (3.9) values were not very dissimilar to those of a normal distribution (0 and 3, respectively). For this reason, and because normality was difficult to be significantly improved, the data were not transformed before parametric tests.

The paired *t*-test showed that mean shoot Zn concentrations were significantly different between LP and HP treatments ($t = 25.78$, df = 196, $P < 0.001$). The means ± SD were 906 ± 480 mg kg^{-1} for the LP treatment and 2805 ± 1261 mg kg^{-1} for the HP treatment. A noticeable change of ranking among genotypes between LP and HP treatments was shown by crossing reaction norms (Supporting Information, Fig. S1). Nevertheless, it seemed that most of reaction norms looked similar and simply showed an increase in Zn concentration differences among genotypes from LP to HP treatment (i.e. a change of scales). This was supported by a significant Spearman rank correlation ($r = 0.49$, $P < 0.001$) between the values of both treatments.

Linkage map

All the 288 individuals from the F_2 progeny were used for the construction of the *A. halleri* × *A. lyrata petraea* linkage map. At a LOD threshold of 4, the 70 markers were assigned to eight linkage groups (Fig. 2) corresponding to the same linkage groups as described in Willems *et al.* (2007). The lengths of each linkage group varied from 51.9 to 85.2 cM, while the marker number varied from 6 to 11 by linkage group. The total length was *c.* 526 cM. The map produced in this study covered 87% of the previous *A. halleri* map (Willems *et al.*, 2007) with an average distance of 8.5 cM between adjacent markers varying from < 1 to 34 cM. The order of the 31 markers shared with Willems *et al.* (2007) was identical in both studies.

Markers in segregation distortion

At a significance threshold of 5%, 46 markers (i.e. 66% of the markers) showed a significant departure from the expected Mendelian ratio (Fig. 2). These markers were located on the eight linkage groups, mainly on LG1, LG2, LG6 and LG7. For all markers on LG1 and half of the markers on

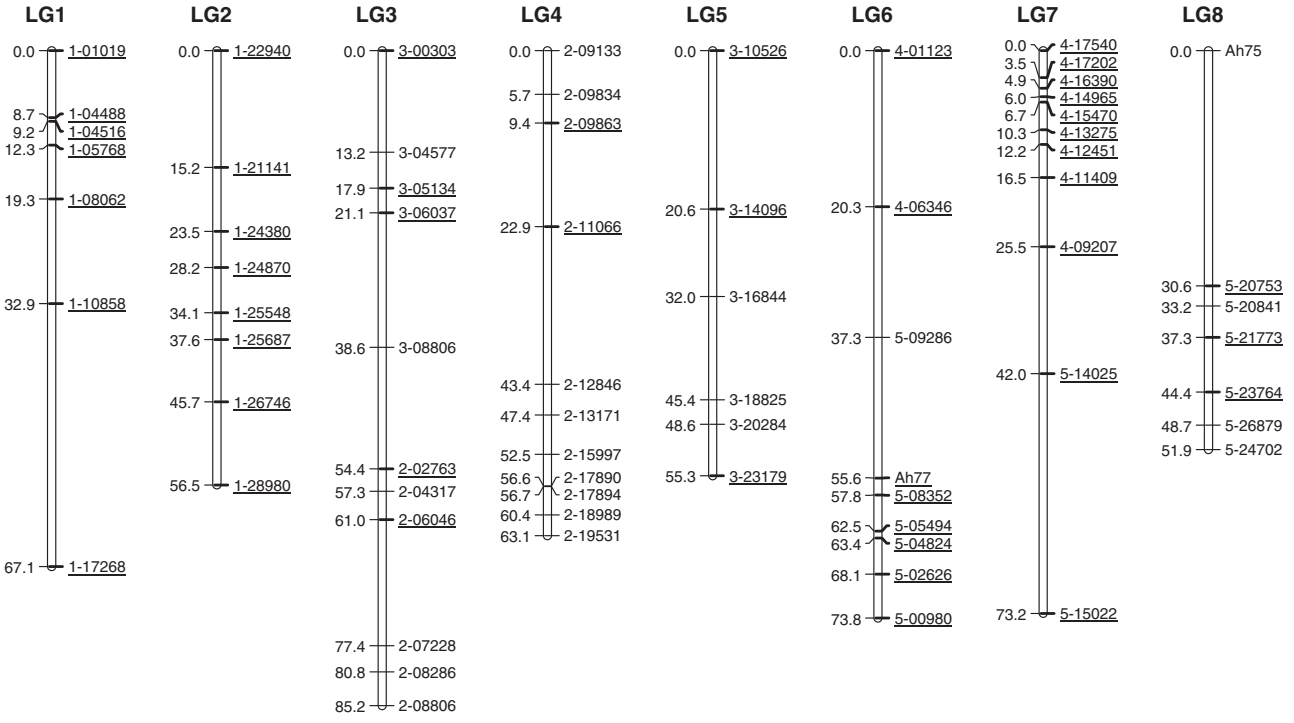

Fig. 2 Linkage map of the *Arabidopsis halleri* × *Arabidopsis lyrata petreae* F_2 progeny constructed with JoinMap 3.0. Markers are labelled on the right of bars by their approximate position on the *Arabidopsis thaliana* genome (chromosome number-position in kb) except for Ah75 and Ah77 (see text for details). Distances on the genetic map are expressed in cM on the left of the bars. Names of loci in segregation distortion are underlined. Ah, *Arabidopsis halleri* microsatellite marker; LG, linkage group.

LG6 and LG7, the progeny was deficient in homospecific *A. halleri* genotype (Table S2). By contrast, for all markers on LG2 and the other part of LG6, the progeny was deficient in homospecific *A. lyrata petraea* genotype (Table S2).

QTL mapping of Zn accumulation in LP and HP treatments

Five QTL regions, located on five linkage groups (LG1, LG3, LG4, LG6 and LG7), were detected by IM and subsequent MQM Mapping as they showed LOD score values above the LOD score threshold (Fig. 3). Five QTL regions that were associated with Zn accumulation in the LP treatment explained together 50.1% of the total phenotypic variance, with most of the variance explained by ZnAcLP-3 on linkage group 7 (Table 1). Three QTL regions were involved in Zn accumulation in the HP treatment. They explained 36.5% of the total phenotypic variance, mostly because of ZnAcHP-1 on linkage group 3 (Table 1). Three QTLs were common to both Zn treatments (ZnAcLP-1/ZnAcHP-1 on LG3, ZnAcLP-2/ZnAcHP-2 on LG6 and ZnAcLP-3/ZnAcHP-3 on LG7), while two additional QTLs were specific to the LP treatment (ZnAcLP-4 on LG1 and ZnAcLP-5 on LG4). Suggestive QTLs were also noticed on chromosomes 2, 4 and 8 as LOD score values (*c.* 3) were close to the LOD threshold (Fig. 3).

For all QTLs in each treatment negative additive effects were obtained, meaning that the *A. halleri* allele increases Zn accumulation compared with the *A. lyrata petraea* allele (Table 2). Dominance effects were either negative or positive, and in some cases variable for a given QTL depending on the parental alleles. This suggests that the parental *A. halleri* alleles can be frequently recessive ($a < 0$ and $d < 0$). Dominance degrees ranged from 0.006 to 2.23. QTLs were rarely additive (three cases among 18) but were often dominant and partially dominant (11 cases). Two QTLs (ZnAcLP-1 and ZnAcLP-3) were slightly over-dominant.

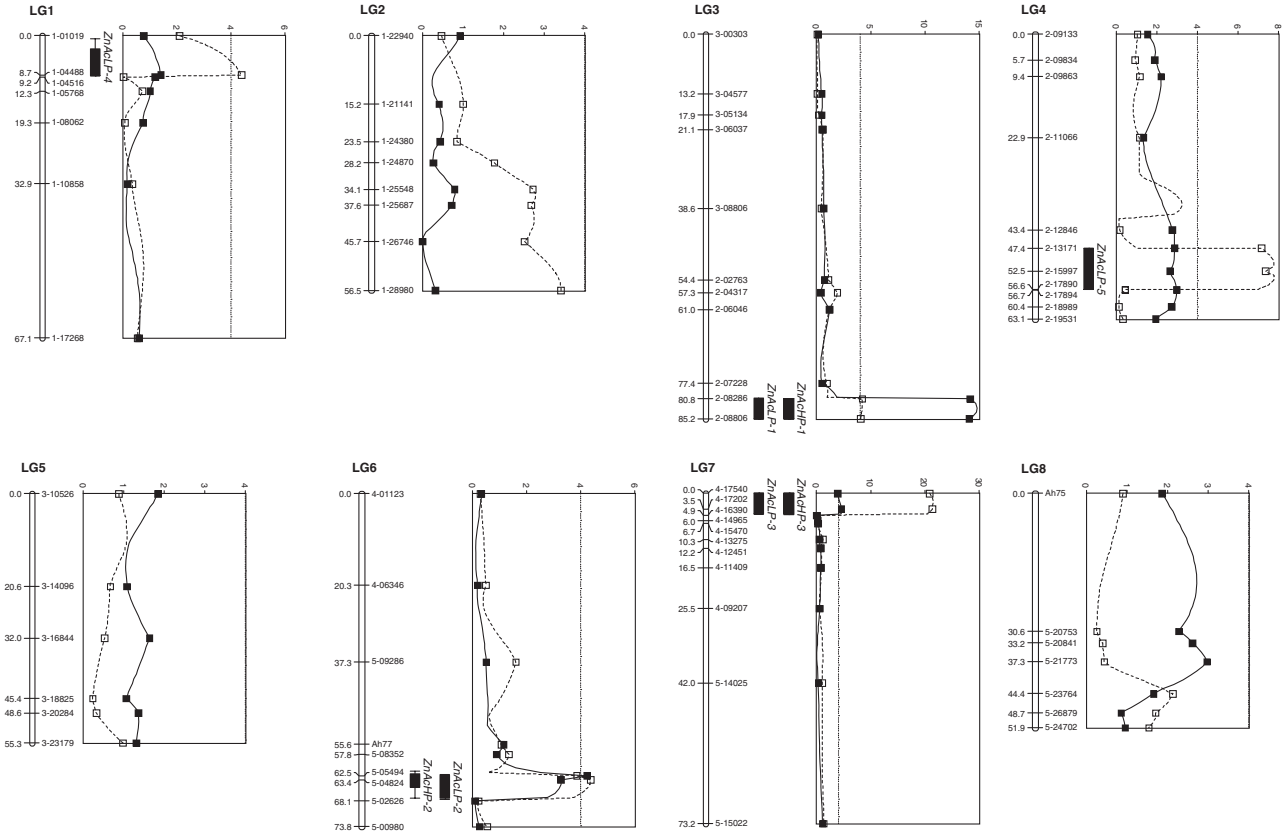

Fig. 3 Quantitative trait locus (QTL) mapping results for Zn accumulation in 'low pollution' (LP) and 'high pollution' (HP) treatments obtained by the Multiple QTL Model (MQM) Mapping method. The eight linkage groups (LG) are represented. Marker names are designated by the position on *Arabidopsis thaliana* chromosomes (except for Ah75 and Ah77 (*Arabidopsis halleri* microsatellite marker), see text for details). On the associated logarithm of odds (LOD) score profiles: horizontal axis, LOD scores; closed squares, HP treatment; open squares, LP treatment. The vertical dotted lines represent the LOD score threshold (4.0) at a 5% error level for QTL detection. The positions of QTLs ('ZnAcLP' for QTL of Zn accumulation in the LP treatment, and 'ZnAcHP' for QTL of Zn accumulation in the HP treatment) are indicated by bars representing the one-LOD support intervals (one LOD score unit on either side of the QTL peak) and whiskers representing the two-LOD support intervals (two LOD score unit on either side of the QTL peak). Bars and whiskers, 95% confidence interval.

Table 1 Summary characteristics of quantitative trait loci (QTLs) detected for zinc (Zn) accumulation in 'low pollution' (LP) and 'high pollution' (HP) treatments

LG/marker[a]	QTL designation[b]	Location[c]	QTL confidence interval[d]	LOD score[e]	R^{2f}
LG1/1-04488	ZnAcLP-4	8.7	1-01019; 1-04488	4.39	4.7
LG3/2-08286	ZnAcLP-1	81.8	2-08286; 2-08806	4.25	4.2
LG3/2-08286	ZnAcHP-1	82.8	2-08286; 2-08806	14.85	24.1
LG4/2-15997	ZnAcLP-5	50.4	2-13171; 2-17894	7.77	8.6
LG6/5-04824	ZnAcLP-2	63.4	5-02626; 5-05494	4.36	4.6
LG6/5-05494	ZnAcHP-2	62.5	5-02626; 5-05494	4.22	5.9
LG7/4-17202	ZnAcLP-3	2.0	4-16390; 4-17540	21.59	28.0
LG7/4-17202	ZnAcHP-3	3.5	4-16390; 4-17540	4.48	6.5

[a]Linkage groups (LGs) where the QTLs were detected and markers at, or closest to, the QTL positions.
[b]QTLs are designed by the trait (Zn accumulation) and the treatment (LP for 'low pollution' treatment and HP for 'high pollution' treatment).
[c]Location of the QTL on each linkage group (in centiMorgans, cM) according to the Multiple QTL Model (MQM) Mapping method.
[d]95% confidence intervals designed by positions of the markers closest to the lower and upper bounds, transferred onto the *Arabidopsis thaliana* genome and expressed as 'chromosome number-position in kb'.
[e]Maximum logarithm of odds (LOD) score value of the linkage group obtained by the MQM Mapping method.
[f]Percentage of variance explained by the QTL.

Table 2 Additive effects, dominance effects, and dominance degrees at the quantitative trait locus (QTL) for Zn accumulation

LG/marker	QTL designation	a[a]	$d_{hal1/lyr2}$[b]	$d_{hal2/lyr1}$[b]	$\|d/a\|_{hal1/lyr2}$[c]	$\|d/a\|_{hal2/lyr1}$[c]
LG1/1-04488	ZnAcLP-4	−192.93	−86.28	−29.46	0.44	0.15
LG3/2-08286	ZnAcLP-1	−115.74	145.84	−24.37	1.26	0.21
LG3/2-08286	ZnAcHP-1	−848.03	476.99	150.02	0.56	0.17
LG4/2-15997	ZnAcLP-5	−200.26	164.68	146.04	0.82	0.72
LG6/5-04824	ZnAcLP-2	−125.22	58.53	−128.74	0.46	1.02
LG6/5-05494	ZnAcHP-2	−481.08	−305.79	−309.43	0.63	0.64
LG7/4-17202	ZnAcLP-3	−179.74	−171.25	401.26	0.95	2.23
LG7/4-17202	ZnAcHP-3	−427.76	2.69	340.12	0.006	0.79

LG, linkage group.
[a]Additive effects of the QTL calculated as $(\mu_{lyr1/lyr2} - \mu_{hal1/hal2})/2$, where $\mu_{hal1/hal2}$ and $\mu_{lyr1/lyr2}$ are the mean concentrations for the homospecific genotypes *Arabidopsis halleri*-1/*halleri*-2 and *A. lyrata*-1/*lyrata*-2 at the markers closest to or at the QTL.
[b]Dominance effects at the QTL corresponding to either $(\mu_{hal1/lyr2} - (\mu_{hal1/hal2} + \mu_{lyr1/lyr2})/2)$ or $(\mu_{hal2/lyr1} - (\mu_{hal1/hal2} + \mu_{lyr1/lyr2})/2)$, where $\mu_{hal1/lyr2}$ and $\mu_{hal2/lyr1}$ are the mean concentrations of the genotypes that are heterospecific *halleri*-1/*lyrata*-2 and *halleri*-2/*lyrata*-1, respectively.
[c]Degree of dominance at the QTL: a QTL is classified as additive ($|d/a| < 0.2$), partially dominant ($0.2 \leq |d/a| < 0.8$), dominant ($0.8 \leq |d/a| < 1.2$), or overdominant ($|d/a| \geq 1.2$).

Interaction tests

Interactions between the QTLs for each treatment were assessed. Even though they were all significant (Table S3), this result has to be interpreted with caution because of very small sample sizes in several genotype classes. Nevertheless, mean phenotype values were always higher in hhxhh genotype classes (when existing) than in llxll genotype classes. Other genotype classes displayed intermediate values. In most cases, a higher number of *A. halleri* alleles resulted in a higher mean accumulation value.

Genotype × environment interactions significantly explained variations in shoot Zn concentration even though the variance component was only 13.6% (Table 3). Likewise, QTL × environment interactions were significant only for ZnAcLP-1/ZnAcHP-1 at marker 2-08286 (F = 13.43, df = 3, $P < 0.001$), ZnAcLP-2/ZnAcHP-2 at both close markers 5-04824 (F = 3.48, df = 2, P = 0.032) and 5-05494 (F = 5.04, df = 2, P = 0.0069), but surprisingly not for ZnAcLP-3/ZnAcHP-3 at marker 4-17540 (F = 0.81, df = 3, P = 0.49). However, the 4-17540 marker showed many missing values (see Table S2) which could bias the result, and hence the occurrence of a QTL × environment interaction could not be totally excluded for the ZnAcLP-3/ZnAcHP-3 QTL.

Discussion

Genetic architecture of Zn hyperaccumulation in *Arabidopsis halleri*

This is the first study to locate QTLs of Zn hyperaccumulation on an *A. halleri* × *A. lyrata petraea* genetic linkage map using soil with two different Zn concentrations. At both Zn

Table 3 ANOVA on Zn accumulation values in *Arabidopsis* in both low pollution and high pollution treatments

Source	df	Type III SS	MS	*F*	*P* > *F*	Variance component (%)
Treatment	1	852824650	852824650	2547.94	< 0.0001	58.8
Genotype	202	608169558	3010740	9.00	< 0.0001	16.5
Treatment × genotype	196	256682696	1309606	3.91	< 0.0001	13.6
Error	595	199152913	334711	11.1		

pollution levels, Zn accumulation was a widely segregating trait in the *A. halleri* × *A. lyrata petraea* F_2 progeny. The continuous and quite normal distribution suggests polygenic inheritance, consistent with previous reports. Indeed, in *A. halleri* as well as *T. caerulescens* metallicolous populations continuous variations for Zn hyperaccumulation were observed (Pollard & Baker, 1996; Macnair, 2002). Pollard *et al.* (2002) suggested that one or a few major genes would control the ability to hyperaccumulate metals, while multiple modifier genes probably regulated the degree of hyperaccumulation. Assunção *et al.* (2003) found a continuous segregation pattern in *T. caerulescens*, and suggested that Zn hyperaccumulation was governed by more than one gene.

The linkage map produced in this study, constructed from 70 markers, was highly congruent with the linkage map reported in Willems *et al.* (2007). It showed the eight linkage groups corresponding to the haploid chromosome number of both parental species with a reasonable number of markers by group (≥ 6) and a relevant average distance between markers (8.5 cM). Strong segregation distortion, as reported on the *A. halleri* × *A. lyrata petraea* BC1 map (Willems *et al.*, 2007), was observed in the F_2 progeny. As, on the genetic linkage map presented in this study, segregation distortion largely involved the same linkage groups as on the BC1 map, and the distorted markers were in most cases linked to markers distorted in the same direction, segregation biases were probably mainly the result of biological reasons rather than genotyping errors. In an interspecific cross, outbreeding depression can be a biological explanation. As an example, genetic combinations between *A. halleri* alleles favoring Zn accumulation and *A. lyrata petraea* alleles decreasing Zn tolerance are possible. Such combinations may have been selected against.

Using this linkage map, this study demonstrated that Zn hyperaccumulation is largely controlled by five QTL regions in the LP treatment (50.1% of the phenotypic variance) on chromosomes 1, 3, 4, 6 and 7 and three QTL regions in the HP treatment (36.5% of the phenotypic variance) on chromosomes 3, 6 and 7. With the exception of chromosome 1, these chromosomes were also reported in previous studies using *A. halleri* × *A. lyrata petraea* progenies to harbor genes involved in Zn hyperaccumulation (Filatov *et al.*, 2006, 2007). Filatov *et al.* (2006) compared the transcriptional profiles of *A. halleri* with those of *A. lyrata petraea*, and also of accumulator F_3 families with those of nonaccumulator F_3 families. They tested the cosegregation with Zn accumulation of markers significantly differing in their expression level. On chromosome 3, the QTL region identified by Filatov *et al.* (2006) was located between the markers 3-05134 and 2-02763, that is, it did not overlap with the QTL region detected in the present study (between 2-08286 and 2-08806). At any rate, on this chromosome, they had no marker located between 2-02763 and 2-08806, and were therefore not able to detect a QTL in this region. The authors also detected a QTL region on chromosome 7 between 4-09207 and 4-16390 markers, which was adjacent to the QTL identified in the present study (between 4-16390 and 4-17540). Filatov *et al.* (2007) constructed a linkage map between *A. halleri* and *A. lyrata petraea* based on 25 markers and assessed Zn hyperaccumulation using hydroponics at two Zn concentrations. They revealed three genomic regions contributing to Zn accumulation, on chromosomes 4, 6 and 7. Some of their markers significantly associated with Zn accumulation (Ahp8, Ahp20, Ahp21, Ahp22 and Ahp23) were located in or close to QTL regions identified in the present study on the same chromosomes. In addition, these authors also detected a possible interaction with metal concentration on chromosome 7, as it was also suggested here at the QTL ZnAcLP-3/ZnAcHP-3.

At all QTLs, *A. halleri* alleles provided higher Zn accumulation values, though with various degrees of dominance. Several *A. halleri* alleles were totally recessive, as suggested by the skewed distribution of F_1 phenotypes towards low Zn accumulation values. As parents' representatives showed different Zn accumulation concentrations, it was expected that several alleles, at one or a few genes, were segregating in *A. halleri* and *A. lyrata petraea*, and thus that several allelic combinations could appear in the F_2 progeny. However, transgressive F_2 phenotypes were rare, suggesting that phenomena such as epistasis or overdominance would be occasional. This was confirmed by the occurrence of only two overdominant QTLs. In addition, epistatic effects estimated through QTL × QTL interactions are still elusive because many genotype classes are poorly represented. Four of the six markers at which QTL × QTL interactions were tested showed significant segregation distortion and, more precisely, a shortage of hal/hal genotypes (Table S2). QTLs for Zn hyperaccumulation detected in this study are consequently largely additive, which is consistent with the observation that the joined effect of several *A. halleri* alleles

at the different QTLs tend to enhance Zn accumulation values. Furthermore, the genotype × environment interaction significantly affected Zn hyperaccumulation, as suggested by significant interaction terms at the QTLs ZnAcLP-1/AnAcHP-1 and ZnAcLP-2/ZnAcHP-2. Surprisingly, while the magnitude of the effect of the QTL ZnAcLP-3/ZnAcHP-3 was highly different in both environments, a significant QTL × environment interaction was not detected at this QTL. As only few reaction norms apparently crossed (Fig. S1), cross-over effects (inversion in the ranking of allelic effects across environments) seemed probable but rare in comparison to scale effects (variation in the magnitude of allelic effects without inversion of ranks) (Juenger *et al.*, 2005). Hence, not surprisingly, the three QTLs identified at both treatments were involved in scale effects, since *A. halleri* alleles increased Zn accumulation in both treatments (additive effects remained negative). No QTL × environment effect was detected at the two treatment-specific QTLs ZnAcLP-4 and ZnAcLP-5, suggesting that phenotypic values at these QTLs in both environments are not contrasted enough, perhaps because of weak statistical power (missing genotype data, segregation distortion).

The occurrence of QTLs identified at either one or both treatments supports distinct genetic models to explain genotype × environment interactions: the allelic sensitivity model (also known as the pleiotropic model) and the gene regulation model (also known as the epistatic model or conditional neutrality) (Juenger *et al.*, 2005; Lacaze *et al.*, 2009). The first model implies that constitutive genes directly exhibit differential expression across environments, while the second one implies that regulatory genes mediate expression of constitutive genes, resulting in their expression only in some environments. Therefore, it cannot be excluded that, in addition to Zn homeostasis genes, regulatory genes may be major determinants in Zn accumulation.

The putative candidate genes

Physiological and biochemical studies showed the importance of the following steps for metal hyperaccumulation: enhanced root uptake, limited storage in the root, active xylem loading, transport by ligands, efficient unloading and storage in the leaves (see Verbruggen *et al.*, 2009 for review; Sarret *et al.*, 2009). Therefore, genes controlling basic mechanisms of Zn homeostasis can be candidate genes for Zn hyperaccumulation. Such candidate genes can be identified in QTL regions according to the method described in Roosens *et al.* (2008b), which takes advantage of the synteny between the *A. halleri* × *A. lyrata petraea* linkage map and the *A. thaliana* genome. Following this method, several genes could be proposed for ZnAcLP-4 and ZnAcLP-5 that showed higher expression levels in *A. halleri* compared with *A. thaliana* (Talke *et al.*, 2006): *ZIP3* and *ZIP4* at ZnAcLP-4, and *SAMS3* and *MTP11* at ZnAcLP-5. In the ZnAcLP-3/ZnAcHP-3 QTL region, *HMA1* was a possible candidate gene, although its expression regulation under different Zn supply is still unknown. Indeed, AtHMA1 is located in chloroplast membrane and affects shoot Zn content (Kim *et al.*, 2009). The most promising candidate was *HMA4*, located in ZnAcLP-1/ZnAcHP-1 QTL. This QTL showed a major effect at high external Zn concentration, and *HMA4* is a gene whose role in Zn homeostasis becomes essential at high Zn concentrations since it encodes a Zn : Cd : Pb pump that ensures effective metal translocation to the shoot after metal uptake and radial symplastic passage through the root (Courbot *et al.*, 2007; Hanikenne *et al.*, 2008).

In addition to the candidate genes presented here, it cannot be excluded that other genes may be actually responsible for Zn hyperaccumulation in *A. halleri*. On the one hand, most of the investigated QTL regions contained several interesting genes with regard to Zn hyperaccumulation, or genes encoding proteins that are not yet characterized in *A. thaliana.* These genes could become pertinent after further functional studies. On the other hand, QTL positions may be imprecise because of genotyping and/or phenotyping errors. Therefore, identification of candidate genes in QTL regions as performed in this study based on synteny between the QTL regions on the *A. halleri* × *A. lyrata petraea* linkage map and the *A. thaliana* genome has to be cautiously interpreted.

Evolution of Zn tolerance and hyperaccumulation

Being an exceptional phenomenon, Zn hyperaccumulation raises several interesting evolutionary questions, such as the nature of the selection pressure, or the relationship with Zn tolerance, which is a clearly adaptive trait. As has been demonstrated for *T. caerulescens* (Assunção *et al.*, 2003; Frérot *et al.*, 2005), this study shows that, also in *A. halleri*, Zn tolerance and hyperaccumulation are partially correlated. Indeed, the major QTL of Zn tolerance on chromosome 3 identified by Willems *et al.* (2007) largely colocalizes with the ZnAcLP-1/ZnAcHP-1 QTL found in the present study. As for Cd and Zn tolerance (Courbot *et al.*, 2007; Willems *et al.*, 2007), *AhHMA4* remains the most likely candidate gene for Zn hyperaccumulation. Indeed, translocation from root to shoot driven by HMA4 may improve Zn tolerance by maintaining low metal concentration in cytoplasm of root cells, and, simultaneously, tends to increase hyperaccumulation in shoots. Such common genetic bases suggest that Zn tolerance and hyperaccumulation may have simultaneously evolved on heavy metal-contaminated soils.

By contrast, while two copies of the vacuolar transporter *MTP1* gene colocalized with two Zn tolerance QTLs (Willems *et al.*, 2007), no *MTP1* gene copy appeared in the QTL regions detected for Zn accumulation. As has been

evidenced in the hyperaccumulator *T. caerulescens* (Küpper *et al.*, 1999), Zn is probably also sequestered in the vacuolar compartment in *A. halleri* (Küpper *et al.*, 2000). Moreover, the role of MTP1 in Zn tolerance and accumulation was recently demonstrated in *Thlaspi goesingense* (Gustin *et al.*, 2009). One possible reason why no QTL at *MTP1* was detected is that variation of *MTP1* expression or function may be present, but is controlled by genetic variation at the locus of a MTP1 regulatory gene. Alternatively, this study may also suggest that, in *A. halleri*, mechanisms other than vacuolar sequestration might be primarily involved in Zn hyperaccumulation, without excluding a role of MTP1, although a less significant one. In support, hyperaccumulation of Zn in leaves of the hyperaccumulator *T. caerulescens* seems to be primarily dictated by root processes, as recently demonstrated by grafting experiments (Guimaraes *et al.*, 2009). Detoxification processes, including vacuolar sequestration, could have evolved only secondarily on metal-contaminated sites, while Zn hyperaccumulation could originate from nonmetalliferous sites. In this regard it would be interesting to perform QTL analyses using progenies involving *A. halleri* individuals from nonmetallicolous populations, as these could reveal original genetic determinants of Zn hyperaccumulation in *A. halleri*.

Acknowledgements

We thank Robert Dron, Angelique Bourceaux and Eric Schmitt for their technical advice and support in taking care of the plants, and Aude Bodin, Andrea Scarpa, and Alicja Kostecka for help in phenotyping and genotyping. We are also very grateful to Monika Mörchen for advice in establishing microsatellite-enriched genomic library in Single Repeat Sequences, and Steve Barnes for introduction of the methodology allowing the definition and use of multiplexes. We thank Vincent Castric, Ronald Oomen and Nancy Roosens for providing primer pairs and/or help in genotyping. We also thank Olivier Loudet, Fabrice Roux, and Maarten Koornneef for scientific discussions and helpful comments on the manuscript. This research was supported by the French Programme ACI/FNS/ECCO (ECODYN, contract no. 04 2 9 FNS) and by the Nord-Pas-de-Calais Region, 'Programme de Recherches Concertées', by the Belgian Science Policy (Interuniversity Attraction Pole Programme VI/33), and the Fonds National de la Recherche Scientifique (grant no. FRFC 2.4.583.08) at the Université Libre de Bruxelles.

References

Antonovics J, Bradshaw AD, Turner RG. 1971. Heavy metal tolerance in plants. *Advances in Ecological Research* 7: 1–85.

Assunção AGL, Ten Bookum WM, Nelissen HJM, Vooijs R, Schat H, Ernst WHO. 2003. A cosegregation analysis of zinc (Zn) accumulation and Zn tolerance in the Zn hyperaccumulator *Thlaspi caerulescens*. *New Phytologist* **159**: 1–8.

Baker AJ. 1981. Accumulators and excluders strategies in the response of plants to heavy metals. *Journal of Plant Nutrition* **8**: 643–654.

Baker AJM, Brooks RR. 1989. Terrestrial higher plants which hyperaccumulate metallic elements – a review of their distribution, ecology and phytochemistry. *Biorecovery* **1**: 81–126.

Baker AJM, McGrath SP, Reeves RD, Smith JAC. 2000. Metal hyperaccumulator plants: a review of the ecology and physiology of a biological resource for phytoremediation of metal-polluted soils. In: Terry N, Bañuelos G, eds. *Phytoremediation of contaminated soil and water*. Boca Raton, FL, USA: Lewis Publishers, 85–107.

Becher M, Talke IN, Krall L, Krämer U. 2004. Cross-species microarray transcript profiling reveals high constitutive expression of metal homeostasis genes in shoots of the zinc hyperaccumulator *Arabidopsis halleri*. *Plant Journal* **37**: 251–268.

Bert V, Bonnin I, Saumitou-Laprade P, de Laguérie P, Petit D. 2002. Do *Arabidopsis halleri* from nonmetalicolous populations accumulate zinc and cadmium more effectively than those from metallicolous populations? *New Phytologist* **155**: 47–57.

Bert V, Macnair MR, De Laguérie P, Saumitou-Laprade P, Petit D. 2000. Zinc tolerance and accumulation in metallicolous and nonmetallicolous populations of *Arabidopsis halleri* (Brassicaceae). *New Phytologist* **146**: 225–233.

Bert V, Meerts P, Saumitou-Laprade P, Salis P, Gruber W, Verbruggen N. 2003. Genetic basis of Cd tolerance and hyperaccumulation in *Arabidopsis halleri*. *Plant and Soil* **249**: 9–18.

Boyd RS, Martens SN. 1992. The *raison d'être* for metal hyperaccumulation by plants. In: Baker AJM, Proctor J, Reeves RD, eds. *The ecology of ultramafic (serpentine) soils*. Andover, UK: Intercept, 279–289.

Broadley MR, Willey NJ, Wilkins JC, Baker AJ, Mead A, White PJ. 2001. Phylogenetic variation in heavy metal accumulation in angiosperms. *New Phytologist* **152**: 9–27.

Brownstein MJ, Carpten JD, Smith JR. 1996. Modulation of non-templated nucleotide addition by tag DNA polymerase: primer modifications that facilitate genotyping. *BioTechniques* **20**: 1004.

Cakmak I. 2008. Enrichment of cereal grains with zinc: agronomic or genetic biofortification? *Plant and Soil* **302**: 1–17.

Churchill GA, Doerge RW. 1994. Empirical threshold values for quantitative trait mapping. *Genetics* **138**: 963–971.

Clemens S. 2001. Molecular mechanisms of plant metal tolerance and homeostasis. *Planta* **212**: 475–486.

Clemens S. 2006. Toxic metal accumulation, responses to exposure and mechanismes of tolerance in plants. *Biochimie* **88**: 1707–1719.

Courbot M, Willems G, Motte P, Arvidsson S, Roosens N, Saumitou-Laprade P, Verbruggen N. 2007. A major quantitative trait locus for cadmium tolerance in *Arabidopsis halleri* colocalizes with HMA4, a gene encoding a heavy metal ATPase1[OA]. *Plant Physiology* **144**: 1052–1065.

Filatov V, Dowdle J, Smirnoff N, Ford-Lloyd B, Newbury HJ, Macnair MR. 2006. Comparison of gene expression in segregating families identifies genes and genomic regions involved in a novel adaptation, zinc hyperaccumulation. *Molecular Ecology* **15**: 3045–3059.

Filatov V, Dowdle J, Smirnoff N, Ford-Lloyd B, Newbury H, Macnair MR. 2007. A quantitative trait loci analysis of zinc hyperaccumulation in *Arabidopsis halleri*. *New Phytologist* **174**: 580–590.

Frérot H, Lefèbvre C, Petit C, Collin C, Dos Santos A, Escarré J. 2005. Zinc tolerance and hyperaccumulation in F_1 and F_2 offspring from intra and interecotype crosses of *Thlaspi caerulescens*. *New Phytologist* **165**: 111–119.

Glenn TC, Schable NA. 2005. Isolating microsatellite DNA loci. *Methods in Enzymology* **395**: 202–222.

Guimaraes MD, Gustin JL, Salt DE. 2009. Reciprocal grafting separates the roles of the root and shoot in zinc hyperaccumulation in *Thlaspi caerulescens*. *New Phytologist* **184**: 323–329.

Gustin JL, Loureiro ME, Kim D, Na G, Tikhonova M, Salt DE. 2009. MTP1-dependent Zn sequestration into shoot vacuoles suggests dual roles in Zn tolerance and accumulation in Zn-hyperaccumulating plants. *Plant Journal* **57**: 1116–1127.

Hanikenne M, Talke IN, Haydon MJ, Lanz C, Nolte A, Motte P, Kroymann J, Weigel D, Krämer U. 2008. Evolution of metal hyperaccumulation required cis-regulatory changes and triplication of HMA4. *Nature* **453**: 391–396.

Jeong J, Guerinot ML. 2008. Biofortified and bioavailable: the gold standard for plant-based diet. *Proceedings of the National Academy of Sciences, USA* **105**: 1777–1778.

Juenger TE, Sen S, Stowe KA, Simms EL. 2005. Epistasis and genotype-environment interaction for quantitative trait loci affecting flowering time in *Arabidopsis thaliana*. *Genetica* **123**: 87–105.

Kim Y-Y, Choi H, Segami S, Cho H-T, Martinoia E, Maeshima M, Lee Y. 2009. AtHMA1 contributes to the detoxification of excess Zn(II) in Arabidopsis. *Plant Journal* **58**: 737–753.

Kolpakov R, Bana G, Kucherov G. 2003. MREPS: efficient and flexible detection of tandem repeats in DNA. *Nucleic Acid Research* **31**: 3672–3678.

Kosambi D. 1944. The estimation of map distances from the recombination values. *Annals of Eugenics* **12**: 172–175.

Küpper H, Lombi E, Zhao FJ, McGrath SP. 2000. Cellular compartmentation of cadmium and zinc in relation to other elements in the hyperaccumulator *Arabidopsis halleri*. *Planta* **212**: 75–84.

Küpper H, Zhao FJ, McGrath SP. 1999. Cellular compartmentation of zinc in leaves of the hyperaccumulator *Thlaspi caerulescens*. *Plant Physiology* **119**: 305–311.

Lacaze X, Hayes PM, Korol A. 2009. Genetics of phenotypic plasticity: QTL analysis in barley, *Hordeum vulgare*. *Heredity* **102**: 163–173.

Larkin MA, Blackshields G, Brown NP, Chenna R, McGettigan PA, McWilliam H, Valentin F, Wallace IM, Wilm A, Lopez R *et al.* 2007. ClustalW and ClustalX version 2. *Bioinformatics* **23**: 2947–2948.

Macnair MR. 1983. The genetic control of copper tolerance in the yellow monkey flower, *Mimulus guttatus*. *Heredity* **50**: 283–293.

Macnair MR. 2002. Within and between population genetic variation for zinc accumulation in *Arabidopsis halleri*. *New Phytologist* **155**: 59–66.

Macnair MR, Bert V, Huitson SB, Saumitou-Laprade P, Petit D. 1999. Zinc tolerance and hyperaccumulation are genetically independant characters. *Proceedings of the Royal Society of London, Biological Series* **266**: 2175–2179.

Macnair MR, Smirnoff N. 1999. Use of zincon to study uptake and accumulation of zinc by zinc tolerant and hyperaccumulating plants. *Communications in Soil Science and Plant Analysis* **30**: 1127–1136.

Malmberg RL, Mauricio R. 2005. QTL-based evidence for the role of epistasis in evolution. *Genetical Research* **86**: 89–95.

Mayer JE, Pfeiffer WH, Beyer P. 2008. Biofortified crops to alleviate micronutrient malnutrition. *Current Opinion in Plant Biology* **11**: 166–170.

Meyer C-L, Kostecka AA, Saumitou-Laprade P, Créach A, Castric V, Pauwels M, Frérot H. 2010. Variability of zinc tolerance among and within populations of the pseudometallophyte *Arabidopsis halleri* and possible role of directional selection. *New Phytologist* **185**: 130–142.

van de Mortel JE, Schat H, Moerland PD, Ver Loren van Themaat E, van der Ent S, Blankestijn H, Ghandilyan A, Tsiatsiani S, Aarts MGM. 2008. Expression differences for genes involved in lignin, gluthatione and sulphate metabolism in response to cadmium in *Arabidopsis thaliana* and the related Zn/Cd-hyperaccumulator *Thlaspi caerulescens*. *Plant, Cell & Environment* **31**: 301–324.

van de Mortel JE, Villanueva LA, Schat H, Kwekkeboom J, Coughlan S, Moerland PD, Ver Loren van Themaat E, Koornneef M, Aarts MGM. 2006. Large expression differences in genes for iron and zinc homeostasis, stress response, and lignin biosynthesis distinguish roots of *Arabidopsis thaliana* and the related hyperaccumulator *Thlaspi caerulescens*. *Plant Physiology* **142**: 1127–1147.

Noret N, Meerts P, Tolrà RP, Poschenrieder C, Barceló D, Escarré J. 2005. Palatability of *Thlaspi caerulescens* for snails: influence of Zn and glucosinolates. *New Phytologist* **165**: 763–772.

Palmgren MG, Clemens S, Williams LE, Krämer U, Borg S, Schjorring JK, Sanders D. 2008. Zinc biofortification of cereals: problems and solutions. *Trends in Plant Sciences* **13**: 464–473.

Pauwels M, Frérot H, Bonnin I, Saumitou-Laprade P. 2006. A broad-scale study of population differentiation for Zn-tolerance in an emerging model species for tolerance study: *Arabidopsis halleri* (Brassicaceae). *Journal of Evolutionary Biology* **19**: 1838–1850.

Pauwels M, Roosens N, Frérot H, Saumitou-Laprade P. 2008a. When population genetics serves genomics: putting adaptation back in a spatial and historical context. *Current Opinion in Plant Biology* **11**: 129–134.

Pauwels M, Willems G, Roosens N, Frérot H, Saumitou-Laprade P. 2008b. Merging methods in molecular and ecological genetics to study the adaptation of plants to anthropogenic metal-polluted sites: implications for phytoremediation. *Molecular Ecology* **17**: 108–119.

Pilon-Smits E. 2005. Phytoremediation. *Annual Review in Plant Biology* **56**: 15–39.

Pollard AJ, Baker AJM. 1996. Quantitative genetics of zinc hyperaccumulation in *Thlaspi caerulescens*. *New Phytologist* **132**: 113–118.

Pollard AJ, Powell KD, Harper FA, Smith JA. 2002. The genetic basis of metal hyperaccumulation in plants. *Critical Review in Plant Sciences* **21**: 539–566.

Reeves RD, Baker AJM. 2000. Metal accumulating plants. In: Raskin I, Ensley BD, eds. *Phytoremediation of toxic metals: using plants to clean up the environment*. New York, NY, USA: Wiley and Sons, 193–229.

Roosens N, Willems G, Godé C, Courseaux A, Saumitou-Laprade P. 2008a. The use of comparative genome analysis and syntenic relationshipsallows extrapolating the position of Zn tolerance QTL regions from *Arabidopsis halleri* into *Arabidopsis thaliana*. *Plant and Soil* **306**: 105–116.

Roosens N, Willems G, Saumitou-Laprade P. 2008b. Using Arabidopsis to explore zinc tolerance and hyperaccumulation. *Trends in Plant Sciences* **13**: 208–215.

Ruggiero MV, Jacquemin B, Castric V, Vekemans X. 2008. Hitch-hiking to a locus under balancing selection: high sequence diversity and low population subdivision at the S-locus genomic region in *Arabidopsis halleri*. *Genetical Research* **90**: 37–46.

Salt DE, Blaylock M, Kumar NPBA, Dushenkov V, Ensley BD. 1995. Phytoremediation: a novel strategy for the removal of toxic metals from the environment using plants. *Biotechnology* **13**: 468–474.

Salt DE, Smith RD, Raskin I. 1998. Phytoremediation. *Annual Review of Plant Physiology and Molecular Biology* **49**: 643–668.

Sarret G, Willems G, Isaure MP, Marcus MA, Fakra SC, Frérot H, Pairis S, Geoffroy N, Manceau A, Saumitou-Laprade P. 2009. Zinc distribution and speciation in *Arabidopsis halleri* × *Arabidopsis lyrata* progenies presenting various zinc accumulation capacities. *New Phytologist* **184**: 581–595.

SAS Institute. 2002. *SAS user's guide: statistics. Version 9.1*. Cary, NC, USA: SAS Institute.

Stuber CW, Edwards MD, Wendel JF. 1987. Molecular marker-facilitated investigation of quantitative trait loci in maize. II. Factors influencing yields and its component traits. *Crop Science* **27**: 639–648.

Talke IN, Hanikenne M, Krämer U. 2006. Zinc-dependent global transcriptional control, transcriptional deregulation, and higher gene

copy number for genes in metal homeostasis of the hyperaccumulator *Arabidopsis halleri*. *Plant Physiology* **142**: 148–167.

Van Ooijen JW, Boer MP, Jansen RC, Maliepaard C. 2002. MapQTL 4.0: software for the calculation of QTL positions on genetic maps. Wageningen, the Netherlands: Plant Research International.

Van Ooijen JW, Voorrips RE. 2001. Joinmap 3.0: software for the calculation of genetic linkage maps. Wageningen, the Netherlands: Plant Research International.

Van Rossum F, Bonnin I, Fénart S, Pauwels M, Petit D, Saumitou-Laprade P. 2004. Spatial genetic structure within a metallicolous population of *Arabidopsis halleri*, a clonal, self-incompatible and heavy-metal-tolerant species. *Molecular Ecology* **13**: 2959–2967.

Verbruggen N, Hermans C, Schat H. 2009. Molecular mechanisms of metal hyperaccumulation in plants. *New Phytologist* **181**: 759–776.

Voorrips RE. 2002. Mapchart: software for the graphical presentation of linkage maps and QTLs. *Heredity* **93**: 77–78.

Weber M, Harada E, Vess C, Roepenack-Lahaye E, Clemens S. 2004. Comparative microarray analysis of *Arabidopsis thaliana* and *Arabidopsis halleri* roots identifies nicotianamine synthase, a ZIP transporter and other genes as potential metal hyperaccumulation factors. *Plant Journal* **37**: 269–281.

Whiting SN, Neumann PM, Baker AJM. 2003. Nickel and zinc hyperaccumulation by *Alyssum murale* and *Thlaspi caerulescens* (Brassicaceae) do not enhance survival and whole-plant growth under drought stress. *Plant, Cell & Environment* **26**: 351–360.

Willems G, Dräger D, Courbot M, Godé C, Verbruggen N, Saumitou-Laprade P. 2007. The genetic basis of zinc tolerance in the metallophyte *Arabidopsis halleri* ssp. *halleri* (Brassicaceae): an analysis of quantitative trait loci. *Genetics* **176**: 659–674.

Willems G, Frérot H, Gennen J, Salis P, Saumitou-Laprade P, Verbruggen N. 2010. Quantitative trait loci analysis of mineral element concentrations in an *Arabidopsis halleri* × *Arabidopsis lyrata petraea* F_2 progeny grown on cadmium contaminated soil. *New Phytologist*, doi: 10.1111/j.1469-8137.2010.03294.x.

Wu R, Stettler RF. 1997. Quantitative genetics of growth and development in Populus. II. The partitioning of genotype × environment interaction in stem growth. *Heredity* **78**: 124–134.

Supporting Information

Additional supporting information may be found in the online version of this article.

Fig. S1 Reaction norms for Zn accumulation values in the 'high pollution' treatment (HP) in comparison to values in 'low pollution' (LP) treatment.

Table S1 List of markers used in linkage map construction.

Table S2 List of markers showing significant segregation distortion in comparison to the Mendelian segregation ratios expected in a F_2 progeny.

Table S3 Mean ± SD of Zn accumulation at the nine genotype classes corresponding to marker by marker interactions for each quantitative trait locus (QTL).

Please note: Wiley-Blackwell are not responsible for the content or functionality of any supporting information supplied by the authors. Any queries (other than missing material) should be directed to the *New Phytologist* Central Office.